

# Blind-spot Analysis of Localization Networks using Second-order Blocking Statistics

Sundar Aditya\*, *Student Member, IEEE*, Andreas F. Molisch\*, *Fellow, IEEE*, Harpreet S. Dhillon†, *Member, IEEE*, Hatim Behairy‡ and Naif Rabeah‡

\* Ming Hsieh Dept. of Electrical Engineering, University of Southern California

† Bradley Dept. of Electrical and Computer Engineering, Virginia Tech

‡ King Abdulaziz City for Science and Technology (KACST), Saudi Arabia

Email: {sundarad, molisch}@usc.edu, hddhillon@vt.edu, {hbehairy, nbnrabeah}@kacst.edu.sa

(Invited Paper)

**Abstract**—The blocking of line-of-sight between anchors and targets by distributed (i.e., non-point) obstacles in an environment can create blind-spots in a localization network if there are an insufficient number of unblocked anchors. The spatial randomness of the obstacle and anchor locations makes it difficult to characterize the blind-spot probability of a network. In this paper, we use tools from stochastic geometry to characterize this randomness. In particular, a homogeneous Poisson point process is used to model the anchor locations and a germ-grain model is employed to represent obstacle locations and shapes. Unlike previous works, which usually assume independent blocking of anchors, we develop tools to handle correlated blocking. Specifically, we use a mixture distribution to approximate the variance of the unshadowed area, which in turn, is used to approximate the blind-spot probability.

**Index Terms**—Stochastic geometry, Correlated blocking, Blind-spot probability, Line-of-sight, Localization

## I. INTRODUCTION

Radio-frequency based localization is becoming increasingly ubiquitous due to the wide range of applications using location-based information. In general, a localization network involves targets and anchors. For passive targets that only reflect incoming signals, time-of-arrival (ToA) based localization is well suited and can provide accuracies in the sub-centimeter range [1]. When no directional information is available, line-of-sight (LoS) between the target and at least three anchors is required for unambiguous ToA-based localization over a 2D plane<sup>1</sup>.

In many environments, the LoS path between two points may be blocked by obstacles such as buildings, furniture etc. Due to the distributed (i.e. non-point) nature of such obstacles, the blocking of LoS from the anchors to a particular target exhibits correlation, in general (e.g., anchors A1 and A2 are blocked to the target by the same obstacle in Fig. 1). A target is said to be in a blind-spot if it has LoS to fewer than three anchors. Ignoring the correlation in LoS blocking events can result in the blind-spot probability of a localization network to be underestimated, e.g., if two anchors, situated close to one another, are each blocked from a target with

probability  $p$ , then the joint blocking probability for the anchors is also approximately  $p > p^2$ . In this paper, we use tools from stochastic geometry to model correlated blocking and its effect on blind-spot events. A stochastic geometry analysis characterizes the performance of a network over an ensemble of environment realizations, instead of a particular snapshot. This leads to a better understanding of system behavior while providing useful design insights. The Poisson point process (PPP) has been used to analyze the performance of different localization networks in a number of recent works [2], [3], [4], while a Boolean model was used to analyze the impact of blocking on urban cellular network performance in [5]. However, the blocking correlation was ignored in all these works. The effect of correlated shadowing on the interference distribution of wireless networks in urban areas was studied in [6] using a Manhattan line process to model building locations.

The main contributions of this work are:

- We model the anchor locations using a homogeneous PPP and the obstacle locations and shapes using a germ-grain model.
- We revisit a known blind-spot probability expression obtained from the independent blocking assumption and derive the conditions under which it underestimates the true blind-spot probability.
- We model correlated blocking by using a mixture distribution to approximate the joint blocking probability of two anchors and use it to compute the first and second moments of the unshadowed area numerically. Using the second-order statistics of the unshadowed area, we approximate the blind-spot probability using a Taylor series expansion.

## II. SYSTEM MODEL

Consider an environment consisting of point targets and distributed obstacles situated in  $\mathbb{R}^2$ . The  $i$ -th obstacle can be represented by the tuple  $(r_i, \phi_i, S_i, \omega_i)$ , where  $(r_i, \phi_i) \in \mathbb{R}^2$  denotes the location of the obstacle in polar coordinates ( $\phi_i \in [0, 2\pi)$ ),  $S_i \subseteq \mathbb{R}^2$  denotes its shape and  $\omega_i$  its orientation.

This work was supported by KACST under grant number 33-878.

<sup>1</sup>we assume 2D localization for convenience. The extension to the 3D case is straightforward.

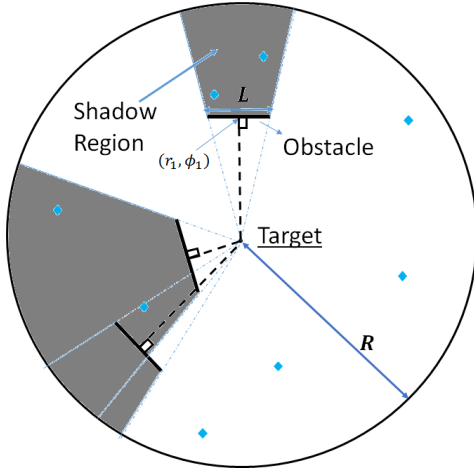


Fig. 1: A localization network consisting of anchors (◆) and obstacles (↘) surrounding a target. The distributed obstacles give rise to correlated blocking. The shadow regions can be viewed as a germ-grain model, where the germs are the obstacle mid-points and the grains are the shaded regions.

The collection of obstacles  $\cup_i (r_i, \phi_i, S_i, \omega_i)$  form a germ-grain model if the following conditions are satisfied [7]:

- (i) The set of points  $\{(r_i, \phi_i)\}$ , known as germs, form a point process in  $\mathbb{R}^2$ .
- (ii) The set  $\{(S_i, \omega_i)\}$ , known as grains are drawn from a family of closed sets  $\mathcal{S} \times \Omega$ .

The obstacles are assumed to be opaque to radio waves; hence, it is reasonable to let  $\mathcal{S}$  be the set of line-segments of length at most  $L$ , where  $L$  is the maximum obstacle length. Without loss of generality, the germs can be chosen to be the mid-points of the line-segments. We assume the germs to be distributed according to a homogeneous PPP with intensity  $\lambda_0$  (i.e., the number of obstacles over a set in  $\mathbb{R}^2$  with area  $A$  is a Poisson random variable with mean  $\lambda_0 A$ ). Throughout this work, we assume a worst-case orientation, i.e., all obstacles lengths are equal to  $L$  and  $\omega_i = \phi_i + \pi/2$  (Fig. 1). Such an orientation ensures maximum shadowing.

A localization network comprising of single-antenna anchors<sup>2</sup> is deployed over  $\mathbb{R}^2$  and we assume the anchor locations to also form a homogeneous PPP, with intensity  $\lambda$ . Due to the stationarity of the PPP, it can be assumed without loss of generality that a target is situated at the origin. A transmit power constraint further restricts our attention to a circular region of radius  $R$ , centered around the target, in which anchors must lie for it to be localized. From the target's perspective, the shadow regions induced by the obstacles form a germ-grain model (Fig. 1), where the area of a grain depends on how far its germ (i.e., the corresponding obstacle mid-point) is from the origin. The blocked anchors are those that lie in the shadow region of an obstacle. Let  $A_v$  denote the area of the unshadowed region.

<sup>2</sup>For simplicity, we assume a monostatic configuration throughout this work, where the anchors are transceivers. All results can easily be extended to the multistatic case as well, with disjoint transmitter and receiver units.

$A_v$  is a random variable that depends entirely on  $L$  and  $\lambda_0$ . The target will be in a blind-spot if there are fewer than three anchors in the unshadowed area. Hence, for anchor intensity  $\lambda$ , the blind-spot probability, conditioned on  $A_v$ , is given by:

$$g(A_v; \lambda) = e^{-\lambda A_v} \left( 1 + \lambda A_v + \frac{(\lambda A_v)^2}{2} \right) \quad (1)$$

The unconditional blind-spot probability,  $b(\lambda)$ , is given by the expression

$$b(\lambda) = \int_0^{\pi R^2} g(A_v; \lambda) f(A_v) dA_v = \mathbb{E}[g(A_v; \lambda)] \quad (2)$$

where  $f(A_v)$  is the distribution of the unshadowed area and  $\mathbb{E}[\cdot]$  is the expectation operator. The distribution of  $A_v$ , while capturing the effect of correlated blocking, is not straightforward to characterize. Hence, simplified approaches need to be developed with the hope of deriving tight bounds and approximations. One of the simplest approaches is to approximate  $b(\lambda)$  by  $g(\mathbb{E}[A_v]; \lambda)$ . In the next section, we show that this is equivalent to assuming independent blocking. We also show that this assumption underestimates the blind-spot probability under certain conditions which typically hold true in most cases. Thus, we propose a new approach to blind-spot probability estimation based on the second-order statistics of  $A_v$ .

### III. BLIND-SPOT PROBABILITY

We define the visibility random variable  $v(r, \phi)$  for the point  $(r, \phi)$  as follows:

$$v(r, \phi) = \begin{cases} 1, & \text{if } (r, \phi) \text{ is not blocked to the origin (target)} \\ 0, & \text{else} \end{cases} \quad (3)$$

$A_v$ , along with its first and second moments, can then be computed by the following expression:

$$A_v = \oint v(r, \phi) r dr d\phi \quad (4)$$

$$\begin{aligned} \mathbb{E}[A_v] &= \oint \mathbb{E}[v(r, \phi)] r dr d\phi \\ &= \oint \mathbb{P}(v(r, \phi) = 1) r dr d\phi \end{aligned} \quad (5)$$

$$\begin{aligned} \mathbb{E}[A_v^2] &= \oint \oint \mathbb{E}[v(r_1, \phi_1) v(r_2, \phi_2)] r_1 dr_1 d\phi_1 r_2 dr_2 d\phi_2 \\ &= \oint \oint \mathbb{P}(v(r_1, \phi_1) = 1; v(r_2, \phi_2) = 1) r_1 dr_1 d\phi_1 \\ &\quad r_2 dr_2 d\phi_2 \end{aligned} \quad (6)$$

where  $\oint := \int_0^{2\pi} \int_0^R$  and  $\mathbb{P}(\cdot)$  is the probability operator. Using the Taylor series expansion about  $\mathbb{E}[A_v]$ , (2) can be approximated as follows:

$$\begin{aligned} b(\lambda) &= \mathbb{E}[g(\mathbb{E}[A_v] + A_v - \mathbb{E}[A_v]; \lambda)] \\ &\approx \mathbb{E}[g(\mathbb{E}[A_v]; \lambda) + g'(\mathbb{E}[A_v]; \lambda)(A_v - \mathbb{E}[A_v]) \\ &\quad + (1/2)g''(\mathbb{E}[A_v]; \lambda)(A_v - \mathbb{E}[A_v])^2] \\ &= g(\mathbb{E}[A_v]; \lambda) + \frac{1}{2}g''(\mathbb{E}[A_v]; \lambda)\sigma_{A_v}^2 \end{aligned} \quad (7)$$

where  $\sigma_{A_v}^2$  is the variance of the unshadowed (visible) area and  $g'(A_v; \lambda)$  and  $g''(A_v; \lambda)$  are the first and second derivatives of  $g(A_v; \lambda)$  with respect to  $A_v$ .

#### A. Independent Blocking

The unblocked anchors can be viewed as a point process obtained by sampling<sup>3</sup> the underlying PPP. For an anchor at  $(r, \phi)$ , the sampling probability equals  $\mathbb{P}(v(r, \phi) = 1)$ . Hence, independent blocking is equivalent to an independent sampling of the anchor PPP, with location-dependent sampling probabilities. As a result, the unblocked anchors form an inhomogenous PPP whose intensity is given by

$$\lambda_{\text{indep}}(r, \phi) = \lambda \mathbb{P}(v(r, \phi) = 1) \quad (8)$$

The blind-spot probability over a circle of radius  $R$  is given by

$$\begin{aligned} b_{\text{indep}}(\lambda) &= e^{-\Lambda(R)} \left( 1 + \Lambda(R) + \frac{\Lambda(R)^2}{2} \right) \\ &= g(\mathbb{E}[A_v]; \lambda) \end{aligned} \quad (9)$$

where  $\Lambda(R) = \oint \lambda_{\text{indep}}(r, \phi) r dr d\phi = \lambda \mathbb{E}[A_v]$  denotes the average number of unblocked anchors over a circle of radius  $R$ .

$g''(A_v; \lambda) = (\lambda^3/2)A_v e^{-\lambda A_v}(\lambda A_v - 2) \geq 0$  when  $\lambda A_v \geq 2$ . Thus,  $g(A_v; \lambda)$  is convex in  $A_v$  for  $A_v \geq 2/\lambda$ . By Jensen's inequality,  $b(\lambda) = \mathbb{E}[g(A_v; \lambda)] \geq g(\mathbb{E}[A_v]; \lambda) = b_{\text{indep}}(\lambda)$  if  $\mathbb{E}[A_v] \geq 2/\lambda$ . Since  $\mathbb{E}[A_v]$  depends on  $\lambda_0$  and  $L$ ,  $b_{\text{indep}}(\lambda)$  is a lower bound for  $b(\lambda)$  over  $\{(\lambda, \lambda_0, L) : \lambda \mathbb{E}[A_v] \geq 2\}$ . From a design perspective, it is desirable to have at least three unblocked anchors, on average (i.e.  $\lambda \mathbb{E}[A_v] \geq 3$ ). Thus, in this regime, it is necessary to take correlated blocking into account to design a localization network that meets a desired blind-spot probability threshold.

#### B. Second-order Statistics of Unshadowed Area

The LoS path to  $(r, \phi)$  is unblocked if and only if there are no obstacle mid-points in the set  $S_v(r, \phi) = \{(\rho, \omega) : \rho \tan |\omega - \phi| \leq L/2, \rho \sec |\omega - \phi| \leq r\}$ , as shown in Fig. 2. Hence,

$$\mathbb{P}(v(r, \phi) = 1) = e^{-\lambda_0 \nu_2(S_v(r, \phi))} \quad (10)$$

$$\nu_2(S_v(r, \phi)) = 2 \int_0^r \rho \min(\arctan(L/(2\rho)), \arccos(\rho/r)) d\rho \quad (11)$$

<sup>3</sup>Equivalently, the blocked anchors can be viewed as a *thinning* of the anchor PPP

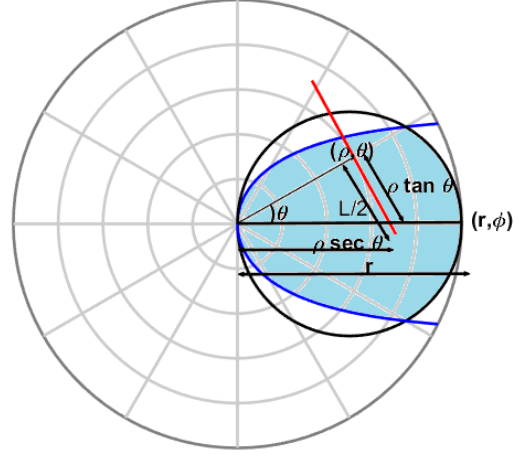


Fig. 2: For  $(r, \phi) = (5, 0)$ , the LoS path to the origin is unblocked if and only if there is no obstacle mid-point in the blue-region.

where  $\nu_2(\cdot)$  denotes the area measure. The average unshadowed area can be computed numerically from (5), (10) and (11). Similarly,

$$\mathbb{P}(v(r_1, \phi_1) = 1; v(r_2, \phi_2) = 1) = e^{-\lambda_0 \nu_2(S_v(r_1, \phi_1) \cup S_v(r_2, \phi_2))} \quad (12)$$

which depends on the extent of overlap between the sets  $S_v(r_1, \phi_1)$  and  $S_v(r_2, \phi_2)$ . The most straightforward case of correlated blocking occurs when the two points lie *behind* one another, i.e.,  $\phi_1 = \phi_2 = \phi$ . In this case,

$$\begin{aligned} \mathbb{P}(v(r_1, \phi) = 1; v(r_2, \phi) = 1) &= \mathbb{P}(v(\max(r_1, r_2), \phi) = 1) \\ &= \mathbb{P}^{(c)}(r_1, r_2) \end{aligned} \quad (13)$$

In general, the overlapping region is difficult to compute. Hence, we approximate the joint probability in (12) (i.e., correlated blocking) using a mixture of  $\mathbb{P}^{(c)}(r_1, r_2)$  and the independent blocking distribution. Therefore,

$$\begin{aligned} \mathbb{P}(v(r_1, \phi_1) = 1; v(r_2, \phi_2) = 1) &\approx (1 - \alpha(\phi_1, \phi_2))\mathbb{P}^{(c)}(r_1, r_2) \\ &\quad + \alpha(\phi_1, \phi_2)\mathbb{P}(v(r_1, \phi_1) = 1)\mathbb{P}(v(r_2, \phi_2) = 1) \end{aligned} \quad (14)$$

where  $\alpha(\phi_1, \phi_2) = \min(|\phi_1 - \phi_2|, 2\pi - |\phi_1 - \phi_2|)/\pi$  is the mixing coefficient.  $\alpha(\phi_1, \phi_2) = 0$  when  $|\phi_1 - \phi_2| = 0$  (maximum blocking correlation) and  $\alpha(\phi_1, \phi_2) = 1$  when  $|\phi_1 - \phi_2| = \pi$  (independent blocking). A linear relationship for  $\alpha$  as a function of  $|\phi_1 - \phi_2|$  is assumed for the sake of simplicity.

$\mathbb{E}[A_v^2]$  can be computed numerically from (13) and (14). Below, we present our numerical results.

#### C. Numerical results and Discussion

We assume  $R = 10\text{m}$  throughout. The impact of correlated blocking is shown in Fig. 3, where we consider two different anchor deployments for fixed  $L$  and  $\lambda_0$  (i.e. constant  $\mathbb{E}[A_v]$ ). In the 'circle' scenario, the anchors are distributed with intensity

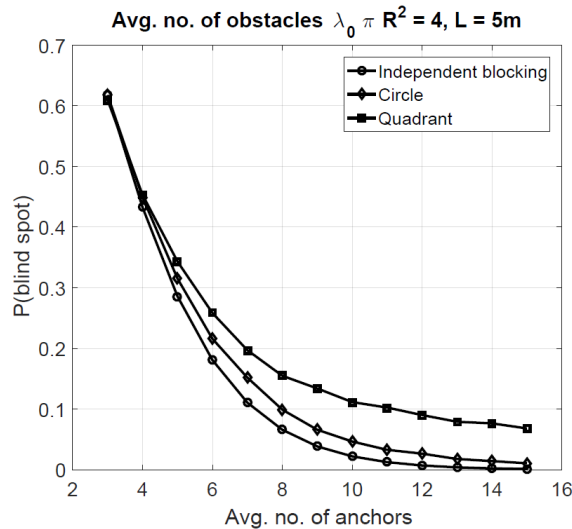


Fig. 3: The impact of correlated blocking is especially significant when the anchors do not have a large angular spread.

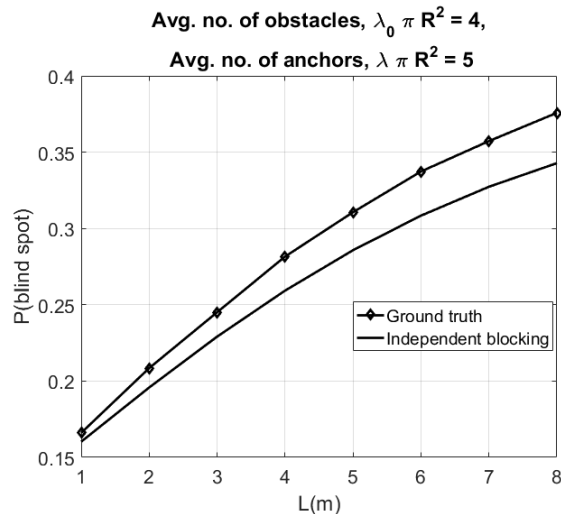


Fig. 4: Larger obstacles induce greater blocking correlation, as a result of which the gap between the two curves increases with  $L$

$\lambda$  over a circle of radius  $R$ , whereas in the ‘quadrant’ case, the anchors locations are restricted to a quadrant with intensity  $4\lambda$ . Thus, in both cases, the average number of unblocked anchors is the same and hence, the independent blocking assumption provides the same result. However, the blind-spot probability for the ‘quadrant’ scenario is higher since the anchors experience highly correlated blocking due to their restricted angular spread.

For fixed  $\lambda$  and  $\lambda_0$ , the effect of obstacle length on blocking is shown in Fig 4, where it can be seen that the true blind-spot probability (labelled ‘ground truth’) is higher than that obtained by assuming independent blocking. As expected, the blind-spot probability increases monotonically in  $L$  for both cases.

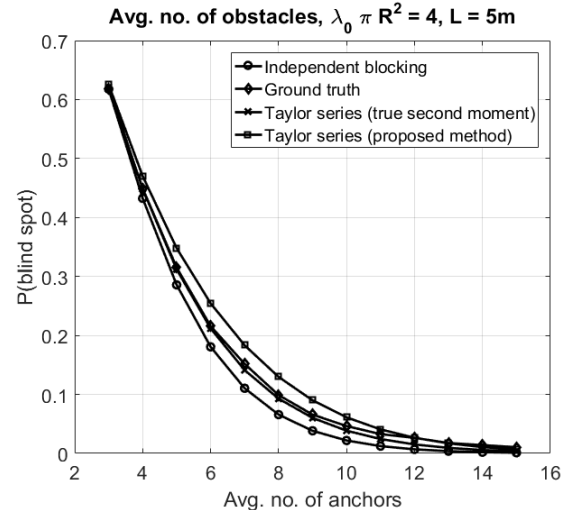


Fig. 5: The mixture distribution overestimates the variance of the unshadowed area.

For  $L = 5m$  and an average of four obstacles, the performance of the Taylor series approximation in (7) is plotted in Fig. 5. The following observations can be made:

- i) As the anchor intensity increases, the blind-spot probability approaches the value obtained by assuming independent blocking. This is intuitive as it is more likely to obtain at least three unblocked anchors from directions that exhibit weak mutual blocking correlation.
- ii) The mixture distribution overestimates the variance of the unshadowed area and consequently, the blind-spot probability because it is only equivalent to independent blocking when the two points are on diametrically opposite ends of the target. In practice however, the independence assumption is usually valid at a smaller angular separation, depending on  $L$  and  $R$ . Refining the mixing coefficient,  $\alpha$ , to provide a better approximation to the blind-spot probability is the subject of future work.

#### IV. SUMMARY

In this paper, we used techniques from stochastic geometry to investigate the effect of obstacle-induced correlated blocking on the blind-spot probability of a localization network. In particular, we used a homogeneous PPP to model the anchor locations and a germ-grain model to represent obstacle locations and shapes. Under these assumptions, the conditions under which the blind-spot probability exceeded the value obtained by assuming independent blocking were derived using Jensen’s inequality. Furthermore, a mixture distribution was used to approximate the variance of the unshadowed area, which was then used to estimate the blind-spot probability using a Taylor series expansion.

#### REFERENCES

- [1] S. Gezici, Z. Tian, G. Giannakis, H. Kobayashi, A. F. Molisch, H. Poor, and Z. Sahinoglu, “Localization via ultra-wideband radios: a look at positioning

- aspects for future sensor networks,” *IEEE Signal Processing Magazine*, vol. 22, no. 4, pp. 70–84, July 2005.
- [2] J. Schloemann, H. S. Dhillon, and R. M. Buehrer, “Towards a tractable analysis of localization fundamentals in cellular networks,” *IEEE Transactions on Wireless Communications*, vol. 15, no. 3, pp. 1768–1782, March 2016.
  - [3] —, “A tractable metric for evaluating base station geometries in cellular network localization,” *IEEE Wireless Communications Letters*, vol. 5, no. 2, pp. 140–143, April 2016.
  - [4] —, “A tractable analysis of the improvement in unique localizability through collaboration,” *IEEE Transactions on Wireless Communications (to appear)*. [Online]. Available: <http://arxiv.org/abs/1507.05681>
  - [5] T. Bai, R. Vaze, and R. W. Heath Jr., “Analysis of blockage effects on urban cellular networks,” *IEEE Transactions on Wireless Communications*, vol. 13, no. 9, pp. 5070–5083, Sept. 2014.
  - [6] F. Baccelli and X. Zhang, “A correlated shadowing model for urban wireless networks,” in *IEEE International Conference on Computer Communications (INFOCOM)*, Hong Kong, April 2015, pp. 801–809.
  - [7] D. Stoyan, S. N. Chiu, W. S. Kendall, and J. Mecke, *Stochastic geometry and its applications*, 3rd ed. Wiley, 2013, ch. 3.